Intermetallics 18 (2010) 36–41

Contents lists available at ScienceDirect

Intermetallics

journal homepage: www.elsevier.com/locate/intermet

Kinetics of isothermal decomposition in polycrystalline β CuAlBe alloys

S. Montecinos [a,b,*], A. Cuniberti [a,b], M.L. Castro [a,b]

[a] Instituto de Física de Materiales Tandil, Universidad Nacional del Centro de la Provincia de Buenos Aires, Pinto 399, 7000 Tandil, Argentina
[b] CONICET, Argentina

ARTICLE INFO

Article history:
Received 25 March 2009
Received in revised form
1 June 2009
Accepted 5 June 2009
Available online 4 July 2009

Keywords:
A. Ternary alloy systems
B. Electrical resistance and other electrical properties
B. Phase transformation
B. Precipitates

ABSTRACT

The kinetics of the microstructural evolution of the metastable β phase during isothermal aging in a Cu–22.60Al–3.26Be (at%) polycrystalline shape memory alloy has been studied by electrical resistivity measurements and microscopical examinations. With an isothermal treatment at around 820 K, the alloy rapidly decomposes into γ_2 phase with dendritic morphology, while between 670 K and 760 K the formation of α' phase followed by the eutectoid decomposition is observed. A TTT diagram was estimated and the stability boundaries of the β phase in the studied alloy were compared with those of other Cu-based shape memory alloys.

1. Introduction

The shape–memory properties exhibited by copper based alloys are due to a thermoelastic martensitic transformation from a high temperature β phase to a martensitic one. The addition of small concentrations of beryllium to the Cu–Al system close to the eutectoidal composition leads to a sharp decrease of the martensitic transformation starting temperature, M_s, around 114 K each 1 at%, without a change in the nature of the transformation ($DO_3 \rightarrow 18R$) [1]. This decrease in M_s enlarges the temperature range at which the martensitic transformation occurs, making Cu–Al–Be alloys an interesting shape memory system. Besides the martensitic transformation, diffusion-controlled phase transformations occur under appropriate conditions. The β phase (disordered bcc) is stable at temperatures higher than 850 K for the eutectoid composition containing approximately 23 at% Al and 3 at% Be [2]. It can be retained at room temperature (RT) by means of suitable cooling, suffering an ordering reaction to a DO_3 structure at temperatures close to 800 K. Under slow cooling rates, below around 100 K/min, the metastable β phase decomposes into the phases α (fcc structure) and γ_2 (Cu_9Al_4 structure), with low and high Al content, respectively [1,2]. Some studies on the Cu–Al β phase decomposition have been reported [3,4]. However, the kinetics of the Cu–Al–Be decomposition has not been studied in detail yet.

The aim of this work was to investigate the kinetics of the microstructural evolution of the metastable β phase during isothermal aging in a Cu–22.60Al–3.26Be (at%) polycrystalline alloy, using electrical resistivity measurements and microscopical examinations. The influence of Be content and grain boundaries is analyzed, and the behaviour of this alloy is compared to that of other β copper-based shape memory alloys.

2. Experimental procedure

The Cu–22.60Al–3.26Be (at%) polycrystalline alloy under study was obtained from Trefimetaux (France), as 15 mm diameter extruded bars. The chemical composition was determined by atomic absorption spectrophotometry. Samples of rectangular section of 3×1.5 mm^2 were cut using an Isomet Low Speed Saw with a diamond disc. Prior to performing the heat treatments, the samples were heated during 5 min at 1073 K in the β field and water quenched at room temperature. The martensite transformation temperature M_s was determined by electrical resistivity, obtaining a value of ~260 K.

Isothermal aging treatments were carried out in a resistive furnace. The electrical resistivity was monitored using a standard four-point probe technique. The temperature was monitored using a chromel-alumel thermocouple spot welded to the sample. For light microscopy (LM) observations, the samples were electropolished in a saturated solution of chromium trioxide in phosphoric

* Corresponding author. Instituto de Física de Materiales Tandil, Universidad Nacional del Centro de la Provincia de Buenos Aires, Pinto 399, 7000 Tandil, Argentina.
E-mail address: dmonteci@exa.unicen.edu.ar (S. Montecinos).

0966-9795/$ – see front matter © 2009 Elsevier Ltd. All rights reserved.
doi:10.1016/j.intermet.2009.06.004

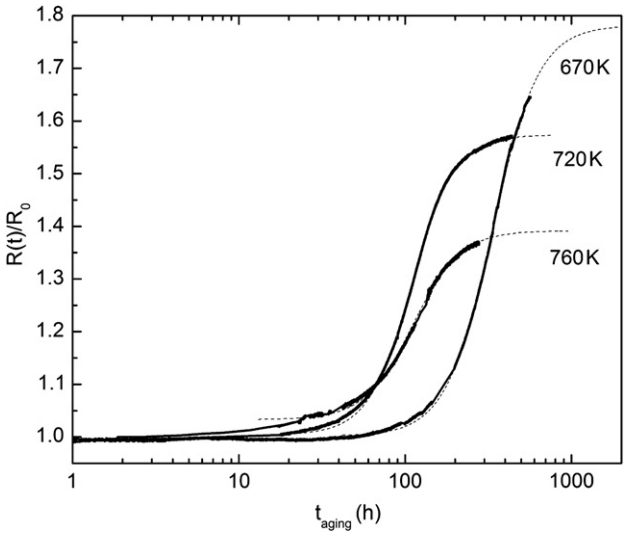

Fig. 1. Electrical resistivity variations against time during isothermal treatments at 670 K, 720 K and 760 K. Dotted lines correspond to the sigmoidal fit.

acid at ~4 V, and suspended for a few seconds in a solution of ferric chloride in order to reveal microstructural details.

3. Results

A phase transformation study during continuous cooling has shown that in this alloy the γ_2 phase is formed between around 873 K and 800 K, while the eutectoid $(\alpha' + \gamma_2)$ decomposition occurs at lower temperatures [2]. Therefore, in order to analyze the kinetics of the β phase decomposition reactions, the following isothermal treatment conditions were chosen:

I. 670 K, 720 K and 760 K, in the $\beta + (\alpha' + \gamma_2)$ field.
II. 820 K, in the $\beta + \gamma_2$ field.

3.1. Decomposition $\beta \rightarrow (\alpha' + \gamma_2)$

Fig. 1 shows the evolution of the electrical resistivity with aging time ($R(t)$) for isothermal treatments at 670 K, 720 K and 760 K. The curves are normalized respect to the initial value of the electrical resistivity for each temperature (R_0) to facilitate the comparison. The isothermal curves present the typical sigmoidal form. After a period in which the resistivity does not vary, a continuous increase is observed until the process decelerates, showing a slope change. The maximum resistivity change increases with decreasing aging temperature. The initial period during which the resistivity does not change can be denominated incubation time, and it is longer for lower temperatures.

Changes in the microstructure were followed by observing at room temperature quenched specimens from selected times along the isothermal curves. Figs. 2–4 show the microstructural evolution with the aging time at each temperature. At 670 K, small nuclei of α' phase are observed after 8 h of aging with a volume fraction around 0.1%. They have the shape of little seeds and produce a considerable distortion in the zones surrounding matrix phase. As the aging time increases, the nuclei lengthen forming thin needles. These shapes would present a better crystallographic adjustment with the matrix, minimizing the superficial tension [5]. Since the α' phase is richer in copper than the β phase [6,7], the matrix surrounding the α' particles is depleted in copper. In those zones, after 48 h aging at 670 K, the presence of γ_2 phase and eutectoid embryos, corresponding to alternated plates of α' and γ_2 phase, is observed. For longer aging times, the volume fraction of the eutectoid increases until almost complete decomposition occurs, and the microstructure obtained after a long time aging is a eutectoid structure with a globular morphology. Grain boundaries do not seem to be preferential nucleation and growing sites.

Similar decomposition processes are observed for higher temperatures, but the α' nuclei and the eutectoid embryos form earlier. As the eutectoid decomposition proceeds, platelets of α' phase grow in the direction of their longer axis and get thicker. After a long aging time of 140 h at 760 K, a eutectoid structure with a laminar

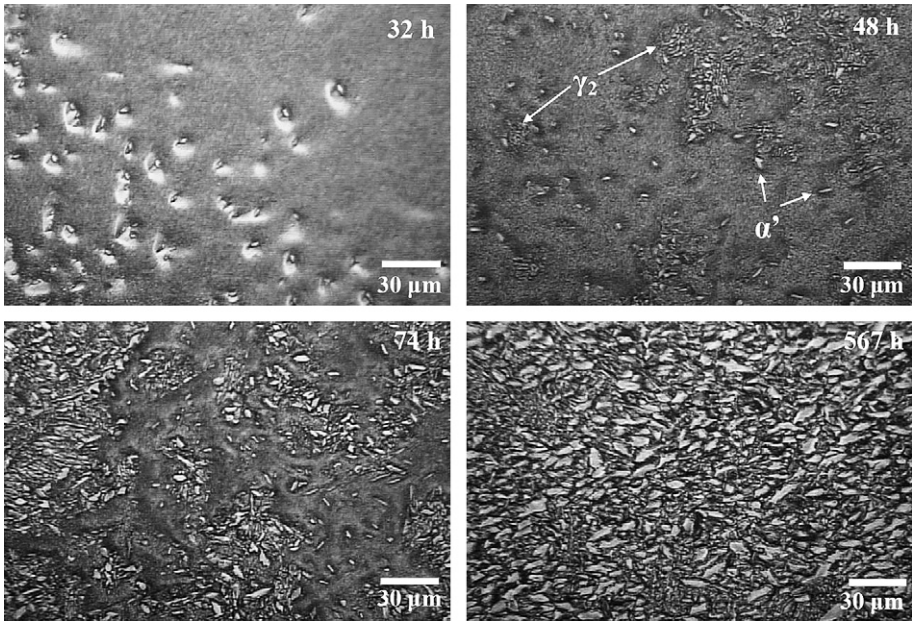

Fig. 2. Micrographs obtained after an isothermal treatment at 670 K. The aging times are indicated.

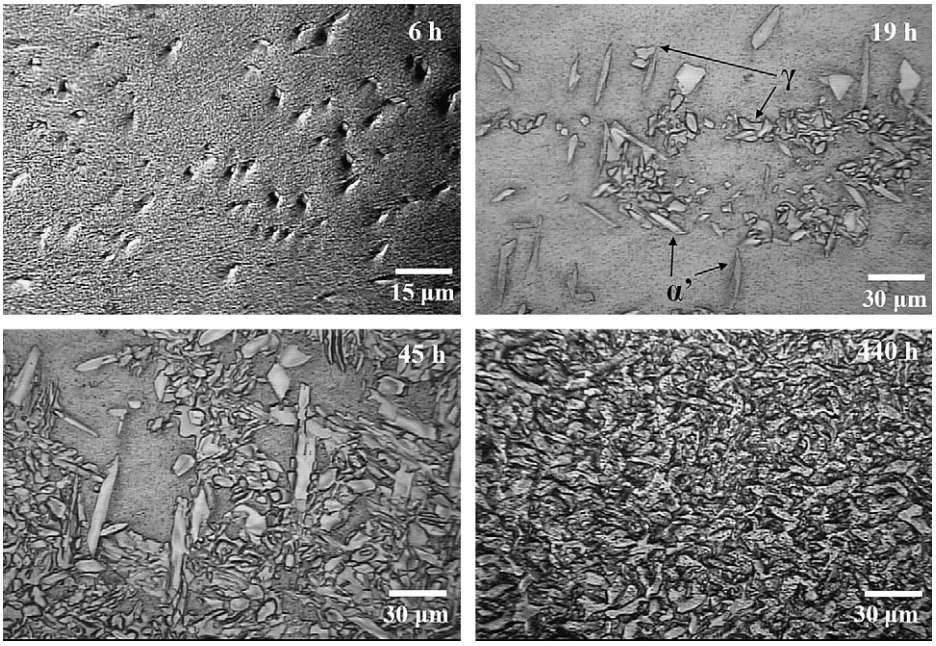

Fig. 3. Micrographs obtained after an isothermal treatment at 720 K. The aging times are indicated.

morphology is observed. It is important to note the increase in the characteristic dimensions of the phases for higher temperatures.

Fig. 5 shows the evolution of the α' precipitates volume fraction (fvα') and mean equivalent diameter (d_{eq}) for the earliest aging times, when the γ_2 phase formation does not occur or is still incipient. fvα' was estimated as the relative area occupied by the precipitates with respect to the total area. d_{eq} was estimated as the diameter which would correspond to the measured precipitates area if they had a circular form. fvα' and d_{eq} increase with aging time and with aging temperature.

When comparing the time involved in the microstructural changes observed by optical microscopy to those related to the electrical resistivity changes, it is possible to infer that the formation and growth of α' phase occur at times in which the resistivity does not present a detectable change, that is during the incubation time. The increase in the electrical resistivity is related to the formation of the eutectoid ($\alpha' + \gamma_2$).

3.2. Decomposition $\beta \rightarrow \gamma_2$

An extremely fast precipitation process, of the order of minutes, takes place at 820 K. The development of γ_2 phase is shown in Fig. 6. After 5 min of aging treatment, the presence of γ_2 precipitates with dendritic morphology is observed. Grain boundaries, as

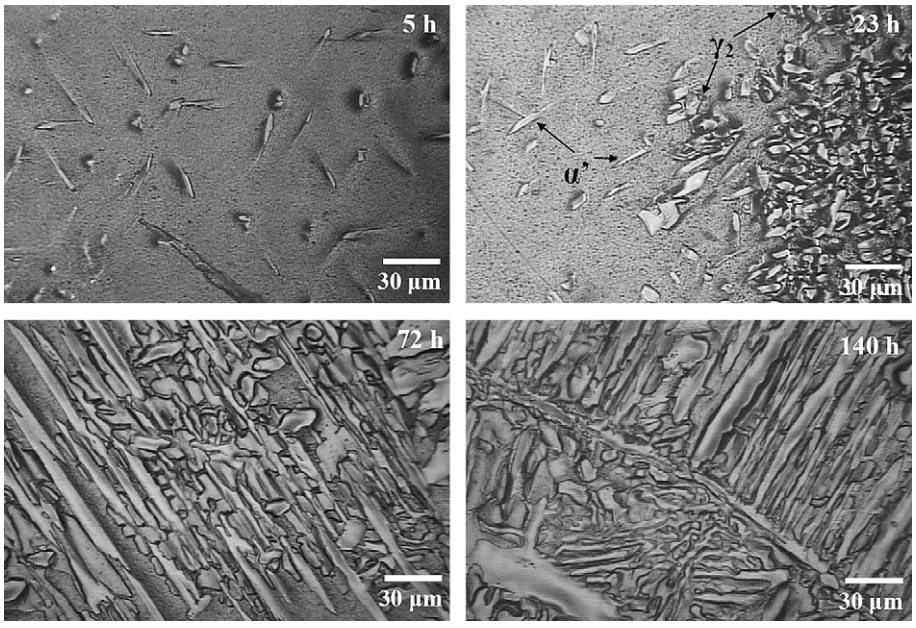

Fig. 4. Micrographs obtained after an isothermal treatment at 760 K. The aging times are indicated.

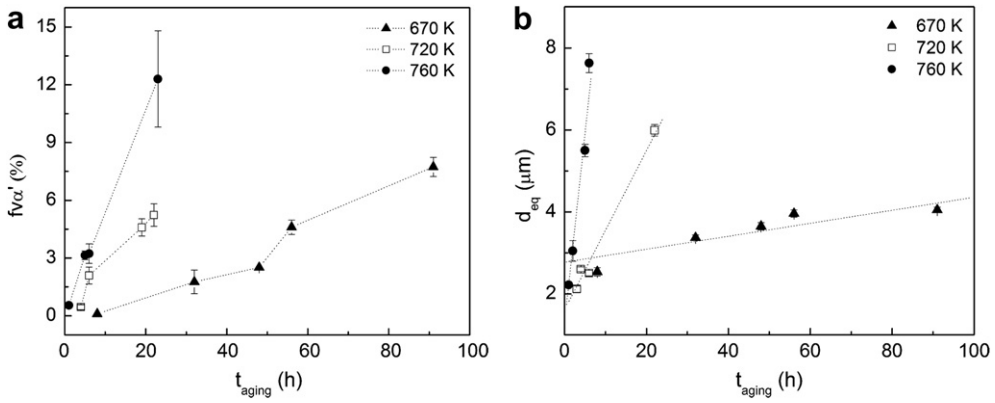

Fig. 5. (a) Volume fraction; and (b) mean size of the α' precipitates formed during isothermal treatments at 670 K, 720 K and 760 K.

fast diffusive paths, appear rapidly decorated by precipitates. The volume fraction ($fv\gamma_2$) increases very fast up to approximately 20% after 8 min of aging and the dendritic structure is accentuated. For the highest $fv\gamma_2$, the dendrite principal arms reach a maximum critical size with around 90 μm of length, and evidences of fragmentation are observed afterwards. After 23 min aging time, almost all the dendrites have been fragmented and for longer times the precipitates have taken globular forms, minimizing the interfacial energy. Due to the disparity of the γ_2 precipitate sizes, an estimation of an average d_{eq} evolution with the aging time was not considered to be representative. Fig. 7 shows that after a maximum at around 8 min, $fv\gamma_2$ decreases slightly. This would be associated with the partial dissolution of the small fragments [8] sized below a critical radius, as well as the difficulty in measuring the submicron precipitates.

The sample needs about 3 min for reaching and stabilizing the temperature at 820 K, and after 510 h the electrical resistivity does not present any change. As the nucleation and growth of γ_2 precipitates are so fast, if these processes produce a resistivity change in the first minutes it could not be observed. However, any later morphological evolution of the γ_2 precipitates is not detected by this technique. It is remarkable that the same observation has been reported in the $\beta \rightarrow \gamma_2$ decomposition in Cu–Zn–Al alloys [9].

4. Discussion

During isothermal treatments at the highest temperature, 820 K, the disordered β phase decomposed into γ_2 precipitates with dendritic form. The dendrite growth as a result of a second phase precipitation in solid–solid transitions has not been extensively studied. It was earlier observed by Mehl and Marzke in 1931 for the γ phase in β Cu–Zn alloys and by Malcolm and Purdy in Cu–Zn–Sn alloys [10]. Castro et al. [11] analyzed the dendrite growth of the γ_2 precipitates in β Cu–Al–Be and Cu–Zn–Al alloys produced by isothermal treatments. The precipitates grow mostly by a diffusive mechanism and the dendrite arms follow well-defined directions as a consequence of the strong dependence of interfacial energy with the crystalline orientation. In a previous work for the studied

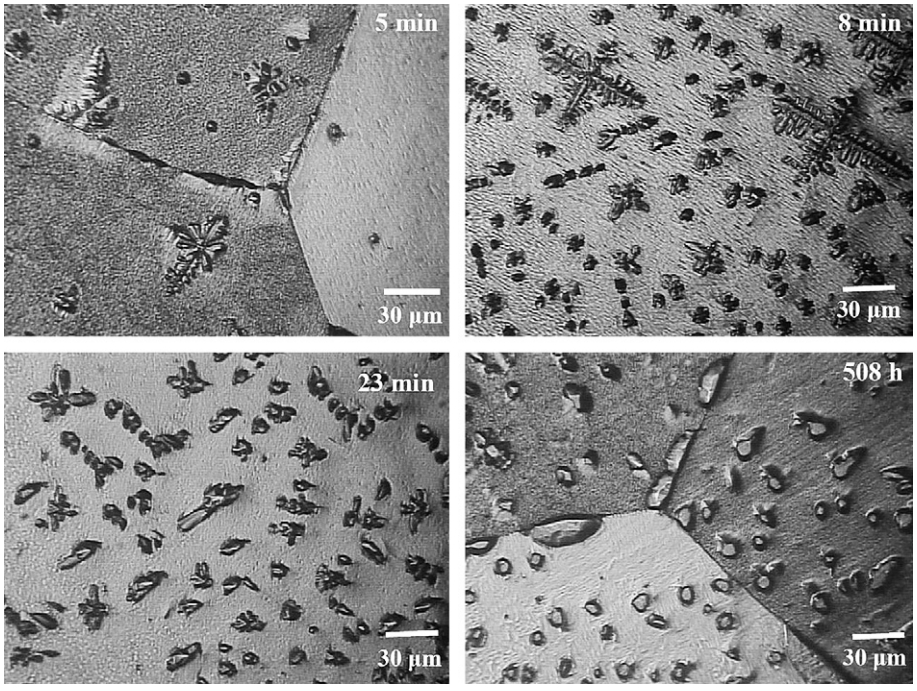

Fig. 6. Micrographs obtained after an isothermal treatment at 820 K. The aging times are indicated.

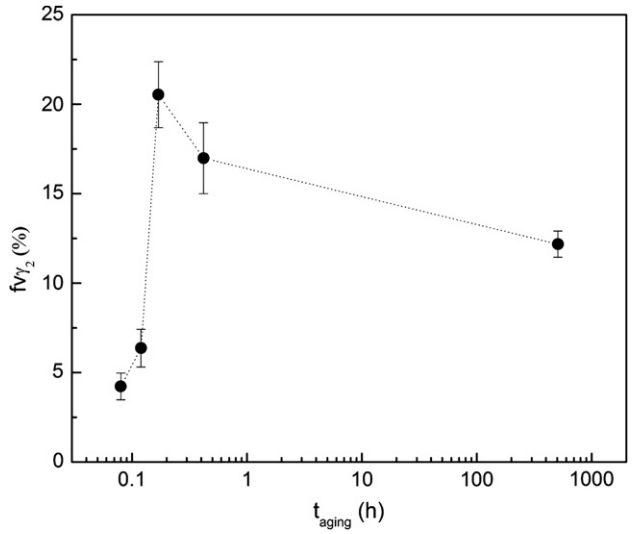

Fig. 7. Volume fraction of the γ_2 precipitates during an isothermal treatment at 820 K. Lines are only referential.

alloy [12], TEM observations have shown an almost perfect continuity between γ_2 and β phases, with no detectable defects like dislocations at the interface, suggesting a good coherency. As has been shown, the nucleation and growth of the γ_2 precipitates are extremely fast in the studied alloy, with an increase in volume fraction around 3% per min during the first 10 min of aging.

For temperatures lower than 800 K, β phase has an ordered DO_3 structure [2,13]. During isothermal treatments between 670 K and 760 K, the sequence of precipitation is β → α′ → eutectoid (α' + γ_2).

The growth kinetics of the α′ precipitates depicted in Fig. 5b follows an almost linear relationship between the mean size and the aging time, with growth rates of 0.02, 0.19 and 0.93 μm/h for aging temperatures of 670 K, 720 K and 760 K, respectively. As has been shown, α′ precipitates grow mainly in one dimension, acquiring needle-like shape. The measured linear growth is consistent with a diffusion controlled mechanism [14,15].

To study the growth kinetics of the eutectoid decomposition, an analysis of the electrical resistivity isothermal curves by means of the Johnson–Mehl–Avrami (JMA) equation [16] was performed. The

Table 1
Values of n and $K(T)$ obtained from Eq. (2) for each aging temperature.

T(K)	n	ln $K(T)$
670	2.01	−11.83
720	2.11	−9.98
760	1.96	−9.42

transformed volume fraction of the eutectoid at a time t_{eq} can be estimated by a parameter y as:

$$y = \frac{R(t_{eq}) - R(t_0)}{R(t_\infty) - R(t_0)} \quad (1)$$

where $t_{eq} = (t - t_0)$ with t_0 and t_∞ the times corresponding to the beginning and the end of the change in the electrical resistivity for each temperature, respectively. Fig. 8 shows the evolution of y versus t_{eq} for the isothermal treatment at 760 K.

The transformed volume fraction of eutectoid can be described by:

$$y = 1 - \exp\left(-K(T)\cdot t_{eq}^{n}\right) \quad (2)$$

where $K(T)$ is the kinetic constant and n is the kinetic exponent that indicates the nature of nucleation and growth. This analysis has been applied to the curves between 10% and 80% of the transformation process. The obtained values of the kinetic parameters are shown in Table 1, and an average of $n = 2.03 \pm 0.04$ was determined. An exponent of 2.0 corresponds to diffusion-controlled growth, for precipitates growing from small dimensions, with decreasing nucleation rate [16].

The temperature dependence of $K(T)$ is generally assumed to be [16]:

$$K(T) = A\cdot\exp(-E/RT) \quad (3)$$

where A is a pre-exponential factor, E is the activation energy for the process, and R is the gas constant. An activation energy of $E = 1.20 \pm 0.24$ eV, associated with the eutectoid decomposition process of a β matrix with pro-eutectoid α′, was obtained. This activation energy is smaller than that measured for the eutectoid decomposition of the β matrix with pro-eutectoid γ of 1.59 eV in Cu–Al–Ni and Cu–Zn–Al alloys [17,18].

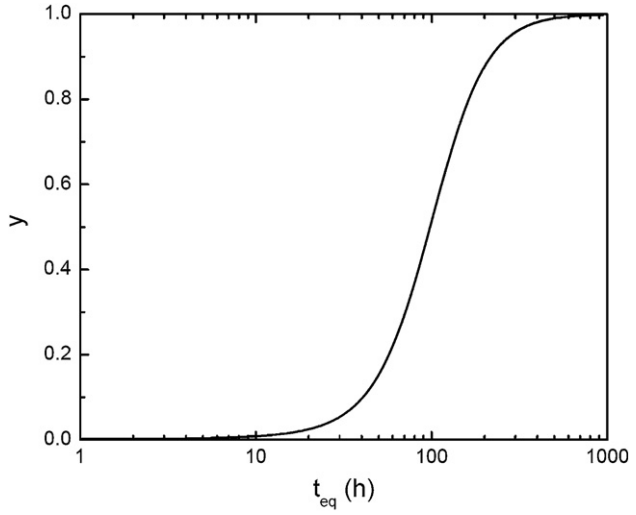

Fig. 8. Evolution of the estimated volume fraction of the eutectoid, y, formed during isothermal treatment at 760 K against the equivalent time (t_{eq}).

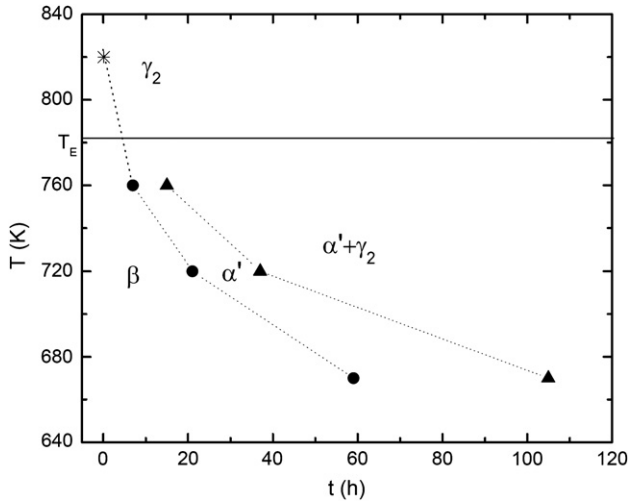

Fig. 9. TTT diagram for the α′ (●) and γ_2 (△) precipitation. See text. Dotted lines are guides to the eyes. T_E corresponds to the eutectoid temperature [1].

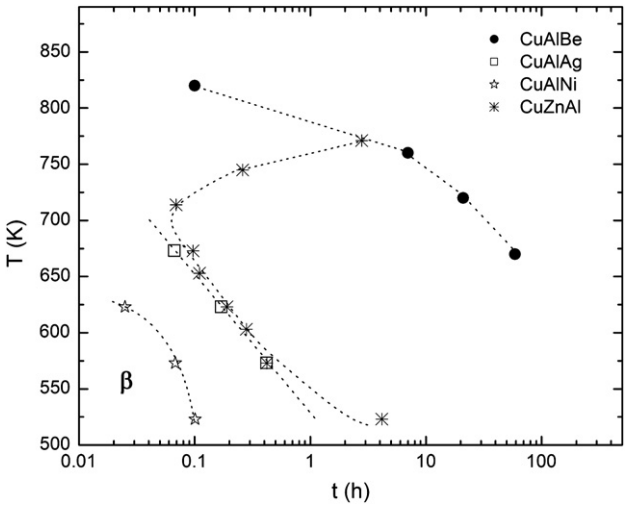

Fig. 10. β phase stability domain for different shape memory alloys. The transformation lines are for transformation start.

For the studied β Cu–22.60Al–3.26Be (at%) alloy, and during isothermal treatments in the eutectoid field, the first precipitated phase formed is α. A similar behaviour has been reported for the Cu–22.71Al–2.57Be (at%) alloy [19]. However, other authors have reported the formation of γ_2 phase as the first precipitate in Cu–22.72Al–3.55Be (at%) [7] and Cu–22Al–3Be (at%) [6] alloys. If attention is focused on the Be content, the sequence of phase transformation does not exhibit a clear trend in the mentioned alloys, and no explanation can be definitively given about which phase will first nucleate. Nevertheless, the formation of α′ or γ_2 phase increases or decreases the aluminum and beryllium content of the matrix respectively [6,7], promoting the formation of the other phase. Thereafter the final microstructure in all case is the eutectoid $(\alpha' + \gamma_2)$. It can be mentioned that the formation of the eutectoid occurs at almost the same time in all the alloys.

The sequence of phase transformations taking place in the studied alloy during isothermal treatments is outlined in a time–temperature–transformation (TTT) diagram, Fig. 9. This diagram was estimated from the results of optical microscopy and electrical resistivity, taking the initiation as the time for which a precipitate volume fraction about 5% was found. The data of the $\beta \rightarrow \alpha'$ and $\beta \rightarrow \gamma_2$ transformations were extrapolated from volume fraction values in Figs. 5a and 7, respectively. The data for the eutectoid $(\alpha' + \gamma_2)$ formation were obtained from the electrical resistivity curves. In the studied range of temperature, the stability domain of the β phase decreases with the temperature. After the α′ precipitates are formed, the eutectoid $(\alpha' + \gamma_2)$ appears faster for higher temperatures. Above the eutectoid temperature ($T_E \sim 780$ K [1]) only γ_2 phase can be observed.

The stability boundaries of the β phase determined in the studied alloy were compared to those reported for Cu–19.2Al–2.1Ag (at%) [20], Cu–23.9Al–4.7Ni–1.6Mn–1.1Ti (at%) [21], and Cu–18.52Zn–14.74Al (at%) [22], Fig. 10. As can be seen, β phase in the studied Cu–Al–Be alloy decomposes at longer aging times and higher temperatures than other shape memory alloys.

The continuous cooling transformation diagram for this alloy has been reported in a previous work [2]. The sequence of phase transformation is similar, but the transformation boundaries lie at lower temperatures in the continuous cooling diagrams than in the isothermal diagrams. This behaviour is similar to that observed in Cu–Al alloys [23].

5. Conclusions

The microstructural evolution of the metastable β phase during isothermal aging treatments in a Cu–22.60Al–3.26Be (at%) shape memory alloy has been studied by electrical resistivity and microscopical examinations.

With an isothermal treatment at around 820 K, the alloy rapidly decomposes into γ_2 precipitates with dendrite forms. Once reached a critical size, dendrite fragmentation occurs and globular form is the observed one for long aging times. Between 670 K and 760 K, the alloy shows the formation of α′ phase followed by the eutectoid decomposition. The electrical resistivity increases when the eutectoid decomposition takes place, while no detectable changes were observed because of the nucleation and growth of either α′ or γ_2 phase. The α′ particles size grows with the aging time in a linear way. The Johnson–Mehl–Avrami (JMA) analysis gives an activation energy of 1.20 eV for the eutectoid decomposition process of a β matrix with pro-eutectoid α′.

A TTT diagram indicates that, in the studied range of temperatures, the stability region of the β phase decreases and the eutectoid forms faster for higher temperatures. The stability boundaries in the studied Cu–Al–Be alloy lie at longer times and higher temperatures than other copper based shape memory alloys.

Acknowledgements

The authors acknowledge the financial support of the ANPCYT, CONICET, the Secretaría de Ciencia y Técnica of the Universidad Nacional del Centro, and the CICPBA, Argentina.

References

[1] Belkahla S, Flores Zuñiga H, Guenin G. Materials Science and Engineering 1993;A169:119–24.
[2] Montecinos S, Cuniberti A, Castro ML, Boeri R. Journal of Alloys and Compounds 2009;467:278–83.
[3] Arruda GJ, Adorno AT, Magnani R, Beatrice CRS. Materials Letters 1997;32:79–84.
[4] Cheetam D, Ridley N. Metallurgical and Materials Transactions 1973;4B(11):2549.
[5] Martin JW, Doherty RD. Stability of microstructures in metallic systems. Cambridge: Cambridge University Press; 1976.
[6] Ochoa-Lara MT, Flores-Zúñiga H, Ríos-Jara D. Journal of Materials Science 2006;41:5455–61.
[7] Castro ML, Romero R. Materials Science and Engineering 2000;A287:66–71.
[8] Castro ML, Romero R. Scripta Materialia 2000;42:157–61.
[9] Castro ML, Romero R. Materials Science and Engineering 1999;A273–275:577–80.
[10] Malcolm JA, Purdy GR. Transactions Metallurgy Society AIME 1967;239:1391–9.
[11] Castro ML, Fornaro O. Revista Materia 2007;12(4):541–8.
[12] Cuniberti A, Montecinos S, Lovey FC. Intermetallics 2009;17:435–40.
[13] Lanzini F, Romero R, Castro ML. Intermetallics 2008;16:1090–4.
[14] Porter DA, Easterling KE. Phase transformations in metals and alloys. London: Chapman and Hall; 2001.
[15] Wu MH, Perkins J, Wayman CM. Acta Metallurgica 1989;37:1821–37.
[16] Christian JW. The theory of transformations in metals and alloys: part I. Oxford: Pergamon Press; 2002.
[17] V. Recarte. PhD thesis, Universidad del País Vasco, Spain; 1997.
[18] M.L. Castro. PhD. thesis, Universidad Nacional del Centro, Argentina; 1999.
[19] Hsu CA, Wang WH, Hsu YF, Rehbach WP. Journal of Alloys and Compounds 2009;474:455–62.
[20] Adorno AT, Silva RAG. Journal of Alloys and Compounds 2004;375:128–33.
[21] Wei ZG, Peng HY, Zou WH, Yang DZ. Metallurgical and Materials Transactions 1997;A28:955–67.
[22] Castro ML, Romero R. Materials Science and Engineering 1998;A255:1–6.
[23] Moon JR, Garwood RD. Journal of the Institute of Metals 1968;96:17–21.